Block-copolymer-induced long-range depletion interaction and clustering of silica nanoparticles in aqueous solution

Sugam Kumar,[1] M.-J. Lee,[2] V. K. Aswal,[1] and S.-M. Choi[2]

[1]*Solid State Physics Division, Bhabha Atomic Research Centre, Mumbai 400 085, India*

[2]*Department of Nuclear & Quantum Engineering, Korea Advanced Institute of Science and Technology, Daejeon 305-701, Republic of Korea*

(Received 14 February 2013; published 29 April 2013)

Small-angle neutron scattering (SANS) has been carried out to examine the block-copolymer-induced depletion interaction of charged silica nanoparticles in aqueous solution. The measurements have been performed on fixed concentrations (1 and 10 wt. %) of anionic Ludox silica nanoparticles having sizes of 8 and 16 nm in the presence of 0.1*M* NaCl and varying concentration of polyethylene oxide–polypropylene oxide–polyethylene oxide P85 $[(EO)_{26}(PO)_{39}(EO)_{26}]$ block copolymer. The presence of the block copolymer induces an attractive depletion interaction between charge-stabilized nanoparticles. The effective interaction of silica nanoparticles is modeled by a combination of two Yukawa potentials accounting for attractive depletion and repulsive electrostatic forces. The depletion interaction is found to be a long-range attraction whose magnitude and range increase with block-copolymer concentration. The depletion interaction is further enhanced by tuning the self-assembly of the block copolymer through the variation of temperature. The increase of the depletion interaction ultimately leads to clustering of nanoparticles and is confirmed by the presence of a Bragg peak in the SANS data. The positioning of the Bragg peak suggests simple-cubic-type packing of particles within the clusters. The scattering from the clusters in the low-Q region is governed by the Porod scattering, indicating that clusters are quite large (order of microns). The depletion interaction is also found to be strongly dependent on the size of the nanoparticles.

DOI: 10.1103/PhysRevE.87.042315 PACS number(s): 82.70.Dd, 61.25.H−, 82.35.Np, 61.05.fg

I. INTRODUCTION

Colloidal dispersions are known to show rich phase behavior and find numerous applications in biotechnology, catalysis, magnetic sealing, optics, photonics, and electronics. The phase behavior strongly depends on interparticle interaction, which can be tuned by varying different solution conditions such as concentration, *p*H, temperature, and ionic strength [1–3]. Many of these phases can be explained by Derjaguin-Landau-Verwey-Overbeek (DLVO) theory governed by the competition of short-range van der Waals attraction and a long-range electrostatic repulsion among the particles [4–6]. However, there are numerous cases where DLVO theory fails and non-DLVO contributions (e.g., hydration and depletion interactions) are required to explain the system behavior [7–9]. For example, there has been recent interest in the clustering of charged colloids including nanoparticles and proteins and it is believed that non-DLVO interaction plays an important role in the phenomena [10,11]. In this case the resultant interaction can be a combination of short-range attraction, long-range attraction, and long-range repulsion [10]. The clustering of proteins at higher concentrations has been observed to arise because of long-range non-DLVO interaction between the protein macromolecules induced by the partial ion clouding around protein molecules [12]. In multicomponent nonadsorbing systems, the depletion interaction is known to play an important role in determining the phase behavior [13]. These depletion interactions govern various interesting kinematic phase transitions (e.g., from individual steel rods to self-assembled polymerlike structures or from vesicles to hybrid core-shell micelles) in different colloidal systems [14,15]. There are, however, very limited studies to model such depletion interactions [16,17].

The depletion force arises in a system consisting of two significantly different sizes of structures (e.g., nanoparticles, micelles, and polymers) due to the exclusion of a nonadsorbed smaller structure from the gap region between larger structures [18]. The resulting concentration difference produces an osmotic pressure imbalance between the gap and bulk, resulting in a net attractive force. The depletion interaction has been mostly considered as short-range attraction and has been found to be applicable to systems that are sterically stabilized with a hard-sphere potential as the repulsive part [16,18]. There have been numerous cases recently where long-range attraction has been observed in charged colloidal systems, leading to their aggregation [7,10,19–21]. In this paper we carry out experiments to examine if the depletion force can be long-range attraction. We observe clustering of charged nanoparticles in the presence of a block copolymer, which can be obtained when the depletion interaction caused by the block copolymer is long-range attraction to overcome long-range repulsion between charged nanoparticles.

Among the various colloidal systems, suspension of nanoparticles in the matrix of polymers provides a model system to study the behavior of depletion interactions [16,22]. In addition to the scientific interest in the depletion-driven phase behavior of the nanoparticle-polymer systems, these systems also have gained industrial and technical attention in fields ranging from biological and medical applications (e.g., targeted drug delivery and diagnostics) to the design of special functional materials [23,24]. The nanoparticles interfaced with polymers have demonstrated utility as protein sensor arrays [25]. Many of these applications require an understanding of interaction parameters in these complex systems. Despite the multidisciplinary interests, it still remains to understand the complex interplay of interparticle forces in these systems and their microstructures.

Herein we study clustering of charged silica nanoparticles as induced by an amphiphilic block copolymer. Block copolymers are used as their self-assembly can be varied

simply by temperature and hence excluded-volume effects for tuning the depletion interaction. Small-angle neutron scattering (SANS) has been used for the characterization due to its unique advantage of contrast variation for the study of these multicomponent systems [17,26–28]. The technique of SANS can also provide information on both the structure and interaction [29]. Data are modeled using a combination of two Yukawa potentials accounting for both attraction and repulsion. The choice of Yukawa potentials can establish the range and strength of the individual parts of the total potential without any predefined assumption [12,30].

II. EXPERIMENT

Electrostatically stabilized 30% (by weight) colloidal suspensions of silica nanoparticles (Ludox LS30 and SM30) and Pluronic P85 block copolymer were obtained from Sigma Aldrich and BASF, respectively. Samples were prepared by dissolving weighted amounts of silica and block copolymer in 15 vol% D_2O in the mixed D_2O/H_2O solvent where the block copolymers are contrast matched. All the measurements were carried out in the presence of $0.1M$ NaCl in order to reduce electrostatic repulsion to be comparable with the depletion attraction where the particle clustering can be observed. Distilled deionized water from a Millipore Milli-Q unit and 99.9% pure D_2O were used for sample preparation. Small-angle neutron scattering experiments were performed using the 40-m SANS instrument at the HANARO at the Korea Atomic Energy Research Institute, Republic of Korea [31]. The wavelength λ of the neutron beam used was 6 Å with a full width half maximum of $\Delta\lambda/\lambda = 12\%$ and the scattered neutrons from the sample were detected using a two-dimensional (1×1)-m^2 detector. Data were collected at two sample-to-detector distances of 2 and 11 m to cover a wave-vector transfer [$Q = 4\pi \sin(\theta/2)/\lambda$, where θ is scattering angle] range of 0.003–0.3 $Å^{-1}$. Samples were held in Hellma quartz cells having a thickness of 2 mm. The measurements were taken at three temperatures: 20 °C, 30 °C, and 40 °C. Data were corrected for background and empty cell contributions and normalized to an absolute cross-sectional unit using standard procedure.

III. SMALL-ANGLE NEUTRON SCATTERING ANALYSIS

In SANS experiments, the coherent differential scattering cross section per unit volume ($d\Sigma/d\Omega$) is measured as a function of Q and can be expressed by [32–34]

$$\frac{d\Sigma}{d\Omega}(Q) = \phi V(\rho_p - \rho_s)^2 P(Q) S(Q) + B, \tag{1}$$

where ϕ is the volume fraction, V is particle volume, ρ_p and ρ_s are scattering length densities of the particles and solvent, respectively, $P(Q)$ is the intraparticle structure factor, $S(Q)$ is the interparticle structure factor, and B is a constant term denoting the incoherent background from the sample. Here $P(Q)$ is determined by the shape and size of the particle and is the square of the single-particle form factor $F(Q)$ as given by

$$P(Q) = \langle |F(Q)|^2 \rangle. \tag{2}$$

For a sphere of radius R, $F(Q)$ is given by

$$F(Q) = \frac{3\{\sin(QR) - (QR)\cos(QR)\}}{(QR)^3}. \tag{3}$$

The factor $S(Q)$ describes the interaction between the particles present in the system and it is the Fourier transform of the pair correlation function for the mass centers of the particles.

The interaction between particles may be attractive or repulsive or a combination of both and can be calculated from double Yukawa potentials accounting for both attraction and repulsion as given by [12]

$$\begin{aligned} U(r) &= \infty \quad \text{for } 0 < r < \sigma \\ &= -K_1 \frac{\exp\{-\alpha_1(\frac{r}{\sigma} - 1)\}}{\frac{r}{\sigma}} \\ &\quad + K_2 \frac{\exp\{-\alpha_2(\frac{r}{\sigma} - 1)\}}{\frac{r}{\sigma}} \quad \text{for } r > \sigma, \end{aligned} \tag{4}$$

where K (in units of k_BT, with k_B the Boltzmann constant and T temperature) is proportional to the magnitude of the potential and $1/\alpha$ is proportional to the range of the potential. Further, $S(Q)$ is obtained by solving the Ornstein-Zernike equation for $U(r)$ in Eq. (4) with a mean spherical approximation closure relation

$$h(r) = c(r) + n \int c(\vec{r} - \vec{r}_1)\, h(r_1)\, d\vec{r}_1, \tag{5}$$

where n is the number density of particles, $c(r)$ is the direct correlation function, $h(r) = g(r) - 1$, and $g(r)$ is the pair correlation function.

For polydispersed systems, $d\Sigma/d\Omega$ in Eq. (1) can be expressed as [35]

$$\frac{d\Sigma}{d\Omega}(Q) = \int \frac{d\Sigma}{d\Omega}(Q,R) f(R) dR + B, \tag{6}$$

where $f(R)$ is the size distribution and is usually accounted for by a log-normal distribution as given by

$$f(R) = \frac{1}{R\,\sigma\,\sqrt{2\pi}} \exp\left[-\frac{\left(\ln\frac{R}{R_{\text{med}}}\right)^2}{2\sigma^2}\right], \tag{7}$$

where R_{med} and σ are the median value and standard deviation, respectively. The mean and median values are related as $R_m = R_{\text{med}} \exp(\sigma^2/2)$. For simplification, the integration in Eq. (4) is carried out over $P(Q)$, whereas $S(Q)$ is calculated for the mean size of the particle.

The data have been analyzed by comparing the scattering from different models to the experimental data. Throughout the data analysis corrections were also made for instrumental smearing. The modeled scattering profiles were smeared by the appropriate resolution function to compare with the measured data [36]. The fitted parameters in the analysis were optimized by means of a nonlinear least-squares-fitting program [37].

IV. RESULTS AND DISCUSSION

Figure 1 shows the SANS data from 1 wt. % of nanoparticles (Ludox LS30) with varying concentration of the block copolymer (P85). In the case of pure silica nanoparticles, the scattering is governed by the intraparticle structure factor $P(Q)$ at 1 wt. % concentration, where the interparticle

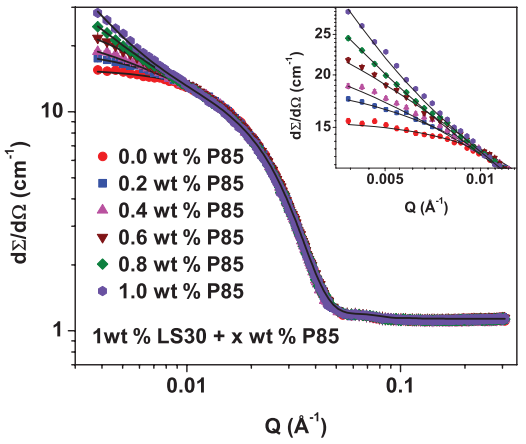

FIG. 1. (Color online) The SANS data of 1 wt. % LS30 silica nanoparticles with varying concentration of P85 block copolymer at 20 °C. The inset highlights the variation in low-Q data.

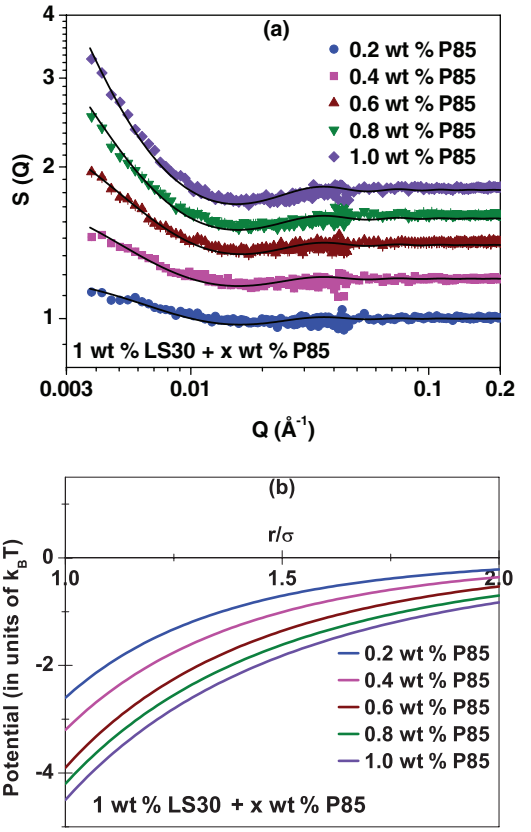

FIG. 2. (Color online) Variation of the (a) structure factor and (b) total interaction potential for 1 wt. % LS30 silica nanoparticles with varying concentration of P85 block copolymer. The data of the structure factor are shifted vertically for clarity.

structure factor $S(Q)$ contribution can be neglected. This assumption has been verified by measuring scattering at lower concentrations, which can be scaled to 1 wt. % concentration by multiplication with the respective concentration factor [38]. The analysis using Eq. (6) provides a mean radius 80 Å with polydispersity 0.2 of silica nanoparticles. It is further observed that there is build up of scattering data in the low-Q region, whereas data overlap in the high-Q region with an increase in block copolymer concentration. There are two possible cases of block copolymer behavior in this system: The block copolymers are either adsorbed on nanoparticles or not absorbed and thus providing depletion force to the nanoparticles. Because block copolymers are contrast matched to the mixed H_2O/D_2O solvent (15% D_2O), their adsorption is expected to show no changes in the scattering pattern [39,40]. This suggests that the changes seen in the scattering pattern (Fig. 1) arise because of interactional changes in the system (the depletion interaction) as a result of the nonadsorption behavior of block copolymers. Also, the systematic buildup of scattering in the low-Q region indicates an increase in the depletion attraction with increasing block-copolymer concentration. This evolution of attraction has been examined by calculating the structure factor by dividing the corresponding data with that of pure nanoparticles and is shown in Fig. 2. The structure factor has been fitted by considering one Yukawa potential taking into account the attractive interaction in the system [12,30]. The fitted parameters are given in Table I. The parameters K_1 and α_1 represent the magnitude and range $(1/\alpha_1)$ of the interaction, respectively. The calculated values of K_1 and α_1 for the van der Waals interaction (short-range attraction) are around 5 and 30, respectively. The significantly lower value of α_1 in Table I as compared to that for the van der Waals interaction suggests the long-range nature of the depletion interaction observed in this system. It should be mentioned that the long-range attraction has also been observed in systems such as charged proteins [10], confined charged colloids [41], and solutions of supramolecular polymers [42]. In the system of charged proteins, long-range attraction is induced by the partial ion clouding around protein molecules [10], whereas the redistribution of electric double layers of ions and counterions is found to be responsible for long-range attraction in confined colloids [7,41]. In the case of supramolecule polymers, long-range attraction is achieved through the depletion interaction by connecting small molecules. Natural processes such as ligand binding to the protein molecules are also observed to be driven through long-range attraction [19]. It is generally believed that the long-range attraction in these systems arises due to manifestation of multibody interactions [7,41].

The measurements discussed so far were taken at 20 °C, where block copolymers are expected to be unimers. Block copolymers at low temperatures [below the critical micelle temperature (CMT)] when both polyethylene oxide (PEO) and polypropylene oxide (PPO) blocks are hydrophilic remain as unimers. The PPO block becomes hydrophobic with an increase in temperature leading to micellization. There exists

TABLE I. Calculated parameters of the attractive depletion interaction in 1 wt. % LS30 nanoparticles as a function of block copolymer concentration.

P85 concentration (wt. %)	K_1 (k_BT)	α_1
0.0		
0.2	2.6	1.8
0.4	3.2	1.5
0.6	3.9	1.3
0.8	4.2	1.1
1.0	4.5	1.0

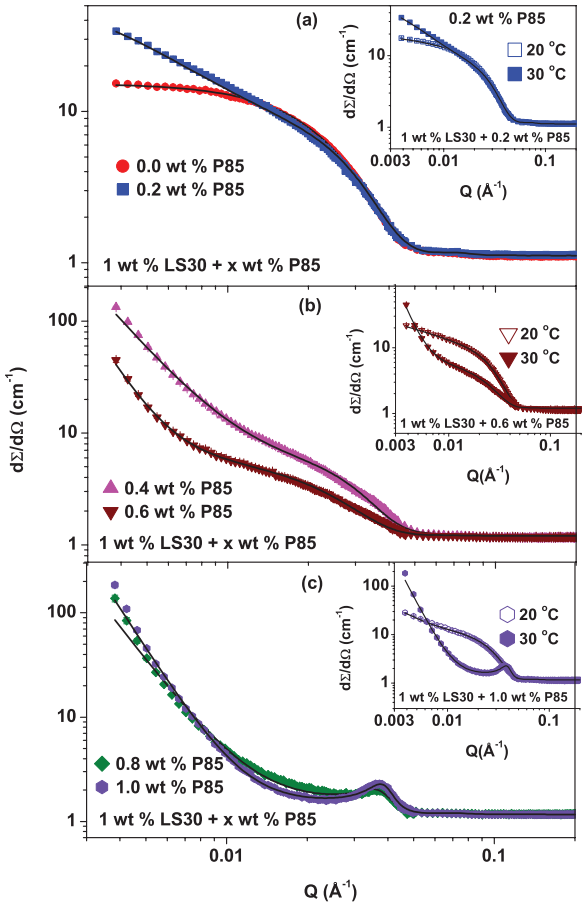

FIG. 3. (Color online) The SANS data of 1 wt. % LS30 silica nanoparticles with varying concentration of P85 block copolymer at 30 °C. The data are divided into three distinct regions [(a) to (c)] of block copolymer concentrations. The inset shows a comparison of data of 30 °C with 20 °C for one block-copolymer concentration in each region.

a temperature range above the CMT where spherical micelles coexist with unimers. At higher temperatures spherical micelles convert to rodlike micelles prior to clouding (phase separation) [43–45]. The effect of self-assembly of block copolymers as induced by temperature on the depletion interaction of nanoparticles (Fig. 3) is examined by increasing the solution temperature (30 °C) significantly above the CMT (25 °C) of the block copolymer [39]. It is observed that the behavior of scattering curves is dramatically altered at higher temperature with an increase in block-copolymer concentration. There is strong buildup of scattering in the low-Q region (<0.1 Å^{-1}) followed by a Bragg peak around $Q = 0.15$ Å^{-1}. This is as a result of enhanced attraction leading to particle aggregation where scattering in the low-Q region arises from the aggregates (clusters) and the Bragg peak from the repeat distance of particles within the aggregates [46]. The data in Fig. 3 are divided in three regions: (i) interacting nanoparticles exist in monomeric form, (ii) coexistence of aggregated with unaggregated (monomeric) nanoparticles, and (iii) all nanoparticles have been aggregated. In region (i), even though the concentration of block copolymers is quite low, the effect on the depletion interaction of an increase in temperature is significantly enhanced (Fig. 3, insets). It is expected that micellization increases the excluded volume, whereas the corresponding decrease in the number density of micelles will decrease it. The net change in the excluded-volume interaction would be a cumulative effect of both of these contributions. Our observations suggest that the increase in excluded volume by the micellization dominates over the decrease in excluded volume by the corresponding decrease in number density of micelles, which enhances the depletion force [18]. In this region, the attractive potential is expected to be less than the average thermal kinetic energy ($1.5k_BT$) at an average distance of the particle, which prevents them from aggregating. The second region corresponds to block-copolymer concentrations when the attractive potential becomes significantly larger than the average thermal kinetic energy and particle aggregation can take place. These data have three different Q-dependent regimes: the low-Q regime governed by the aggregates of particles, the intermediate-Q regime suggesting aggregates coexisting with unaggregated nanoparticles, and the high-Q regime dominated by the incoherent background. The coexistence of aggregated and nonaggregated particles arises because of the polydispersity of particles where smaller particles (less total charge) will undergo aggregation prior to larger particles. The decrease in the scattering intensity in particular in the intermediate-Q range indicates the decrease in number density of unaggregated particles (increase in number density of aggregated particles). In region (iii) of

TABLE II. Calculated parameters of the depletion interaction and resultant structures for 1 wt. % silica nanoparticles as a function of block copolymer concentration at 30 °C. (a) The system is characterized by individual nanoparticles undergoing depletion interaction. (b) The system consists of nanoparticle aggregates coexisting with individual nanoparticles. (c) The system consists of nanoparticle aggregates.

(a)

P85 concentration (wt. %)	K_1 (k_BT)	α_1
0.2	10.0	1.7

(b)

P85 concentration (wt. %)	Surface fractal dimension D_s	Fraction of nonaggregated particles (%)
0.4	2.9	78
0.6	2.8	60

(c)

P85 concentration (wt. %)	Surface fractal dimension D_s	Particle-particle distance d (Å)	Volume fraction within the aggregates φ
0.8	2.5	170	0.4
1.0	2.0	170	0.4

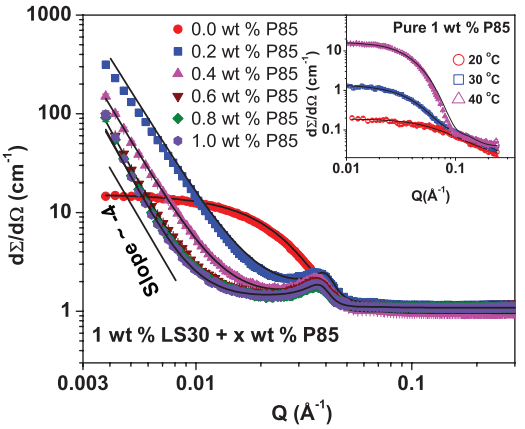

FIG. 4. (Color online) The SANS data of 1 wt. % LS30 silica nanoparticles with varying concentration of P85 block copolymer at 40 °C. The inset shows the effect of temperature on the 1 wt. % P85 block copolymer system.

the block-copolymer concentration, the increase in depletion with an increase in block-copolymer concentration gives rise to ordered aggregates reflected in the Bragg peak observed around $Q = 0.04$ Å^{-1}. The corresponding average distance between the particles ($d \sim 2\pi/Q$) having values similar to the particle size suggests a simple-cubic-type packing of the particles within the aggregates [47]. The scattering from aggregates is fitted by the sum of a power-law behavior of fractal aggregates and contribution from particles within the aggregates. The fitted parameters are given in Table II. The magnitude of depletion interaction is enhanced on the self-assembly (micellization) of block copolymers at higher temperature. The particle aggregation induced by depletion interaction is characterized by a surface fractal $\sim Q^{-(6-D_s)}$, where the fractal dimension D_s decreases with an increase in block-copolymer concentration. The higher propensity to aggregate at higher block copolymer concentration is expected to lead to smooth surfaces and hence smaller fractal dimension [4]. The Bragg peak is fitted through $S(Q)$ by employing a hard-sphere potential in the Percus-Yevick approximation.

Figure 4 shows SANS data of the results of a depletion interaction at 40 °C. The subsequent increase in the size of the micelles at this temperature results in the increase in the excluded-volume effect causing an increase in depletion attraction. This increase in attraction leads to the nanoparticle aggregation at 40 °C even at the lowest block-copolymer concentration, unlike the case of 30 °C. All SANS data at 40 °C show a Bragg peak whose position remains independent ($Q \sim 0.04$ Å^{-1}) of the block-copolymer concentration, whereas the scattering profile becomes narrower in the low-Q region with an increase in block-copolymer concentration. This can be understood in terms of the increase in the size of the aggregates while maintaining their ordered structure. The fitted parameters of aggregates of nanoparticles are given in Table III(a). The surface fractal dimension of aggregates in accord with the increase in size of the aggregate decreases as expected with the increase in block-copolymer concentration. The volume fraction of the particles within aggregates has a value around 0.4, which is significantly less than that for an ordered simple cubic structure (0.54) and can be expected for deviations from a perfect ordering of particles (i.e., short-range-ordered structures).

The strong temperature dependence of the depletion interaction in the present system arises as a result of enhanced micellization of block copolymers with an increase in temperature, which is examined in the inset Fig. 4. The data of a pure block-copolymer solution (prepared in D_2O) show an increase in scattering intensity (proportional to the scattering volume) with temperature, indicating the increasing size of the block-copolymer self-assembly. These block copolymer micelles can be modeled as consisting of a hydrophobic core with Gaussian chains (hydrophilic part) attached to it [48]. The dependence of calculated micellar parameters on temperature are given in Table III(b), which clearly shows an increase in micellization (volume fraction and size) with temperature [49].

All the above measurements (Figs. 1–4) have been carried out at 1 wt. % concentration of silica nanoparticles to

TABLE III. (a) Structural parameters of nanoparticle aggregates as induced by a block copolymer at 40 °C. (b) Parameters of the micellar structure of the 1 wt. % P85 block copolymer at different temperatures. The calculated value of the radius of gyration of the unimer is 22 Å.

(a)

P85 concentration (wt. %)	Surface fractal dimension D_s	Particle-particle distance d (Å)	Volume fraction within the aggregates φ
0.0			
0.2	2.5	170	0.37
0.4	2.3	170	0.38
0.6	2.0	170	0.40
0.8	2.0	170	0.40
1.0	2.0	170	0.40

(b)

Temperature (°C)	Micellar fraction ϕ (%)	Core radius R_c (Å)	Aggregation number N	Radius of gyration of PEO chain R_{gc} (Å)
15	0			
30	15	36.0	52	15.0
45	100	38.3	63	15.0

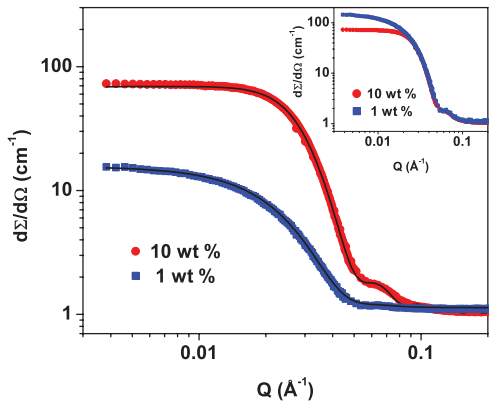

FIG. 5. (Color online) The SANS data of pure 1 and 10 wt. % of LS30 nanoparticles systems. The inset shows data after scaling.

consider the system dilute for repulsive interactions. The SANS measurements were also carried out at a much higher concentration of silica nanoparticles (10 wt. %) to examine the competition of attractive depletion with repulsive electrostatic interactions in these systems. Figure 5 shows a comparison of SANS data of pure 1 and 10 wt. % pure silica nanoparticles. The scaling of two results by the concentration factor shows significant differences in these data sets in the low-Q region. The fall of scattering in the low-Q region at higher particle concentration is observed because of the repulsive interaction between particles. The data are fitted with a repulsive Yukawa potential. The data of 10 wt. % silica nanoparticles in the presence of block copolymers are shown in Fig. 6. These data suggest attractive depletion competing with repulsive electrostatic with the former interaction dominating with increasing block-copolymer concentration. The data are fitted with two Yukawa potentials accounting for the two interactions [12]. The fitted parameters are given in Table IV. The potential parameters K_2 and α_2 for repulsive interaction are fixed for all the systems as obtained from pure 10 wt. % silica nanoparticle solution. The magnitude and range increase with increasing block-copolymer concentration. The magnitude has the same order in both the higher and lower particle concentrations.

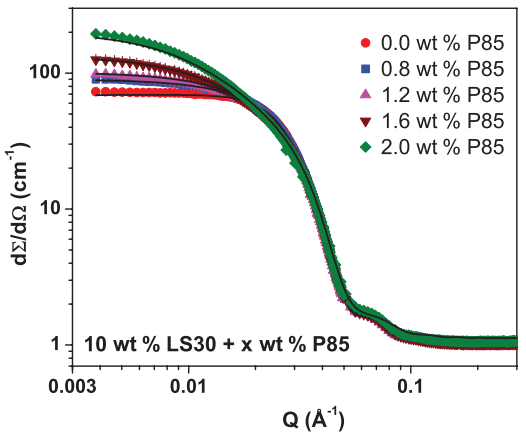

FIG. 6. (Color online) The SANS data of 10 wt. % LS30 silica nanoparticles with varying concentration of P85 block copolymer at 20 °C.

TABLE IV. Calculated parameters of the total interaction potential of 10 wt. % LS30 nanoparticles as a function of block copolymer concentration.

P85 concentration (wt. %)	(k_BT)	$K_1\ \alpha_1$	(k_BT)	$K_2\ \alpha_2$
0.0			3.0	9.0
0.8	2.0	7.0	3.0	9.0
1.2	2.4	6.5	3.0	9.0
1.6	3.5	5.6	3.0	9.0
2.0	4.5	5.2	3.0	9.0

However, the range is found to decrease significantly with an increase in particle concentration. This implies that the depletion interaction becomes less effective in resulting particle aggregation on increasing particle concentration [18]. This effect is depicted in Fig. 7, where SANS data of 1 and 10 wt. % nanoparticles with 1 wt. % block copolymer are compared at different temperatures. It can be clearly seen that there is suppression in the attractive interaction followed by suppressed aggregation at higher temperature in the case of higher nanoparticle concentration.

The variations in the calculated structure factor and total interaction potential for 10 wt. % nanoparticles in the presence

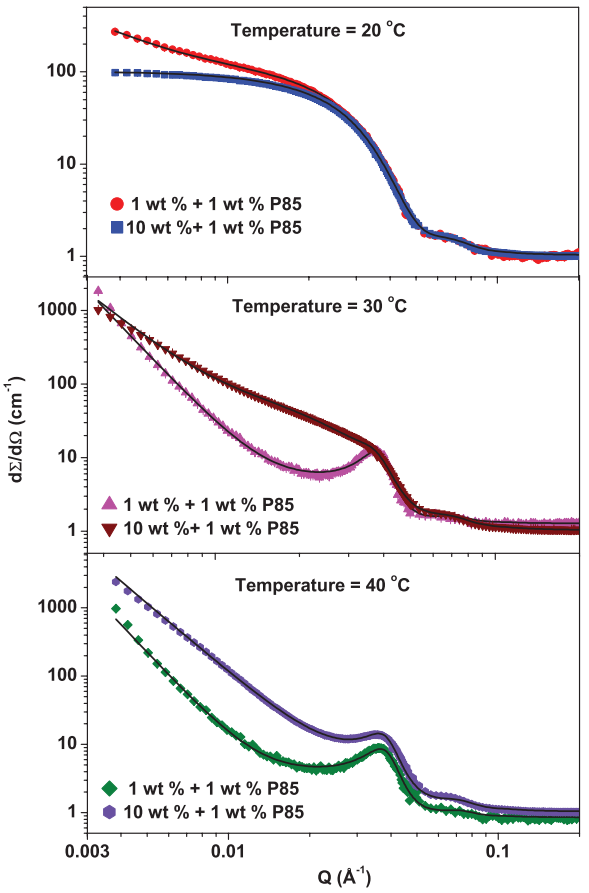

FIG. 7. (Color online) Comparison of SANS data of 1 and 10 wt. % nanoparticles with 1 wt. % block copolymer at different temperatures.

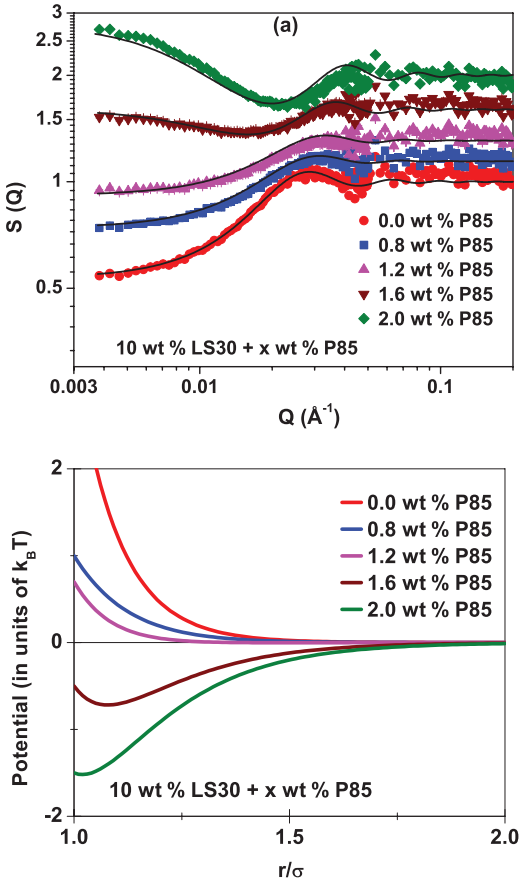

FIG. 8. (Color online) Variation of the (a) structure factor and (b) total interaction potential for 10 wt. % LS30 silica nanoparticles with varying concentration of P85 block copolymer. The data of the structure factor are shifted vertically for clarity.

of increasing block-copolymer concentration at 20 °C are plotted in Fig. 8. The signature of the resultant potential can be observed from the low-Q behavior of the structure factor, in particular, through $S(Q = 0)$ determined by the isothermal compressibility [34]. The variation of the structure factor thus shows the repulsive nanoparticle system becoming attractive with an increase in block-copolymer concentration. The correlation peak shifting towards the higher-Q value with increasing block-copolymer concentration indicates the reduction in the interparticle separation with increasing depletion attraction [50]. The fitted total interaction potentials corresponding to structure factors [Fig. 8(a)] are plotted in Fig. 8(b). It is found that up to 1.2 wt. % of block-copolymer concentration the total potential is dominated by the repulsive component, whereas a prominence of depletion interactions is experienced at higher block-copolymer concentrations (>1.6 wt. %) [18].

The depletion force depends on the excluded volume, which can be varied in different ways depending on the components and solution conditions [18]. We have already seen that an increase in excluded volume on micellization of block copolymers with increasing temperature enhances depletion interaction. The excluded volume can also be tuned by the size of nanoparticles and therefore it is expected to play an important role in determining the depletion force.

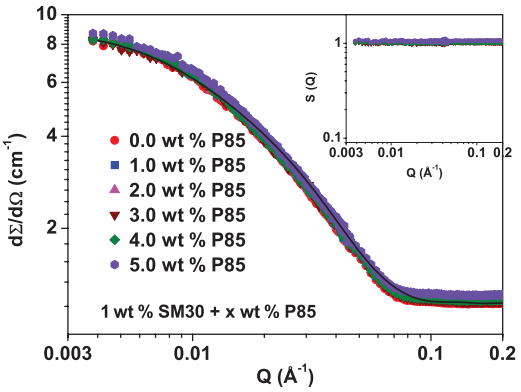

FIG. 9. (Color online) The SANS data of 1 wt. % SM30 silica nanoparticles with varying concentration of P85 block copolymer at 20 °C. The inset shows the corresponding structure factors.

The SANS data of smaller Ludox SM30 nanoparticles (80 Å) with varying block-copolymer concentration are shown in Fig. 9. Unlike the case of larger nanoparticles (Fig. 1), the data in Fig. 9 do not show any significant change, even up to a very large concentration (5 wt. %) of block copolymers. There is in fact no depletion interaction observed for the smaller nanoparticles. The calculated structure factor (inset of Fig. 9) more or less remains the same with increasing block-copolymer concentration. The absence of a depletion interaction may be understood in terms of a decrease in the excluded-volume effect with a decrease in the size of nanoparticles.

V. CONCLUSION

The evolution of the structure and interaction in an aqueous solution of charged silica nanoparticles and amphiphilic block copolymers has been studied by SANS. The presence of amphiphilic block copolymers induces a depletion interaction between charged silica nanoparticles leading to particle clustering. The depletion interaction has been modeled using an attractive Yukawa potential whose range has been found to be much larger than the van der Waals attraction. The aggregation of charged nanoparticles is observed as a consequence of the dominance of the depletion interaction over long-range electrostatic repulsion. The magnitude and range of the depletion interaction can be tuned by the size of the nanoparticles and concentration of block copolymers as well as by the self-assembly of block copolymers through the solution temperature. The particles in a depletion interaction form large clusters and are characterized by the surface fractal structure.

ACKNOWLEDGMENTS

M.-J.L. thankfully acknowledges support from a National Research Foundation grant funded by the MEST of Korea (Grant No. 2011-0031931). The authors acknowledge the HANARO Neutron Research Center at the Korea Atomic Energy Research Institute for providing beam time at the 40-m SANS instrument.

[1] M. D. Determan, L. Guo, C.-T. Lo, P. Thiyagarajan, and S. K. Mallapragada, Phys. Rev. E **78**, 021802 (2008).

[2] J. E. Klijn, M. C. A. Stuart, M. Scarzello, A. Wagenaar, and J. B. F. N. Engberts, J. Phys. Chem. B **111**, 5204 (2007).

[3] H.-S. Jang, C. Do, T.-H. Kim, and S.-M. Choi, Macromolecules **45**, 986 (2012).

[4] A. J. Chinchalikar, V. K. Aswal, J. Kohlbrecher, and A. G. Wagh, Chem. Phys. Lett. **542**, 74 (2012).

[5] P. Attard, Curr. Opin. Colloid Interface Sci. **6**, 366 (2001).

[6] W. Chen, S. Tan, Y. Zhou, T.-K. Ng, W. T. Ford, and P. Tong, Phys. Rev. E **79**, 041403 (2009).

[7] W. R. Bowen and A. O. Sharif, Nature (London) **393**, 663 (1998).

[8] A. M. Molina, J. G. I. Armenta, E. G. Tovar, R. H. Alvarez, and M. Q. Pérez, Soft Matter **7**, 1441 (2011).

[9] A. Stradner, H. Sedgwick, F. Cardinaux, W. C. K. Poon, S. U. Egelhaaf, and P. Schurtenberger, Nature (London) **432**, 492 (2004).

[10] Y. Liu, E. Fratini, P. Baglioni, W.-R. Chen, and S.-H. Chen, Phys. Rev. Lett. **95**, 118102 (2005).

[11] S. Kumar, V. K. Aswal, and J. Kohlbrecher, Langmuir **27**, 10167 (2011).

[12] Y. Liu, W.-R. Chen, and S.-H. Chen, J. Chem. Phys. **122**, 044507 (2005).

[13] V. J. Anderson, E. H. A. de Hoog, and H. N. W. Lekkerkerker, Phys. Rev. E **65**, 011403 (2001).

[14] J. Galanis, R. Nossala, and D. Harries, Soft Matter **6**, 1026 (2010).

[15] W. Agut, D. Taton, A. Brûlet, O. Sandre, and S. Lecommandoux, Soft Matter **7**, 9744 (2011).

[16] X. Ye, T. Narayanan, P. Tong, J. S. Huang, M. Y. Lin, B. L. Carvalho, and L. J. Fetters, Phys. Rev. E **54**, 6500 (1996).

[17] X. Ye, T. Narayanan, P. Tong, and J. S. Huang, Phys. Rev. Lett. **76**, 4640 (1996).

[18] C. N. Likos, Phys. Rep. **348**, 267 (2001).

[19] T. Sato, T. Komatsu, A. Nakagawa, and E. Tsuchida, Phys. Rev. Lett. **98**, 208101 (2007).

[20] M. P. Fernández, A. M. Jordá, and J. C. Fernández, J. Chem. Phys. **134**, 054905 (2011).

[21] G. M. Kepler and S. Fraden, Phys. Rev. Lett. **73**, 356 (1994).

[22] A. I. Chervanyov, Phys. Rev. E **83**, 061801 (2011).

[23] Q. H. Zeng, A. B. Yu, and G. Q. Lu, Prog. Polym. Sci. **33**, 191 (2008).

[24] G. Schmidt and M. M. Malwitz, Curr. Opin. Colloid Interface Sci. **8**, 103 (2003).

[25] C. C. You, O. R. Miranda, B. Gider, P. S. Ghosh, I. B. Kim, B. Erdogan, S. A. Krovi, U. H. F. Bunz, and V. M. Rotello, Nat. Nanotechnol. **2**, 318 (2007).

[26] D. I. Svergun and M. H. J. Koch, Rep. Prog. Phys. **66**, 1735 (2003).

[27] S. Chodankar, V. K. Aswal, J. Kohlbrecher, R. Vavrin, and A. G. Wagh, Phys. Rev. E **79**, 021912 (2009).

[28] S. Chodankar, V. K. Aswal, J. Kohlbrecher, R. Vavrin, and A. G. Wagh, Phys. Rev. E **77**, 031901 (2008).

[29] S. Kumar and V. K. Aswal, J. Phys.: Condens. Matter **23**, 035101 (2011).

[30] A. Shukla, E. Mylonas, E. Cola, S. Finet, P. Timmins, T. Narayanan, and D. Svergun, Proc. Natl. Acad. Sci. USA **105**, 5075 (2008).

[31] Y.-S. Han, S.-M. Choi, T.-H. Kim, C.-H. Lee, and H.-R. Kim, J. Appl. Cryst. **40**, S442 (2007).

[32] J. B. Hayter and J. Penfold, Colloid Polym. Sci. **261**, 1022 (1983).

[33] S.-H. Chen and T. L. Lin, in *Methods of Experimental Physics*, edited by D. L. Price and K. Skold, Vol. 23 B (Academic, New York, 1987), p. 489.

[34] E. W. Kaler, J. Appl. Cryst. **21**, 729 (1988).

[35] J. S. Pedersen, Adv. Colloid Interface Sci. **70**, 171 (1997).

[36] J. S. Pedersen, J. Appl. Cryst. **24**, 893 (1991).

[37] P. R. Bevington, *Data Reduction and Error Analysis for Physical Sciences* (McGraw-Hill, New York, 1969).

[38] S. Kumar, V. K. Aswal, and J. Kohlbrecher, Langmuir **28**, 9288 (2012).

[39] P. Alexandridis and T. A. Hatton, Colloids Surf. A **96**, 1 (1995).

[40] Y. Lin and P. Alexandridis, J. Phys. Chem. B **106**, 10834 (2002).

[41] J. C. Crocker and D. G. Grier, Phys. Rev. Lett. **77**, 1897 (1996).

[42] W. Knoben, N. A. M. Besseling, and M. A. Cohen Stuart, Phys. Rev. Lett. **97**, 068301 (2006).

[43] K. Mortensen, J. Phys.: Condens. Matter **8**, A103 (1996).

[44] G. E. Newby, I. W. Hamleya, S. M. Kingb, C. M. Martinc, and N. J. Terrilld, J. Colloid Interface Sci. **329**, 51 (2009).

[45] B. Hammouda, Eur. Polym. J. **46**, 2275 (2010).

[46] D. Aili, P. Gryko, B. Sepulveda, J. A. G. Dick, N. Kirby, R. Heenan, L. Baltzer, B. Liedberg, M. P. Ryan, and M. M. Stevens, Nano Lett. **11**, 5564 (2011).

[47] T. G. Shin, D. Müter, J. Meissner, O. Paris, and G. H. Findenegg, Langmuir **27**, 5252 (2011).

[48] J. S. Pedersen, J. Appl. Cryst. **33**, 637 (2000).

[49] D. Ray, V. K. Aswal, and J. Kohlbrecher, Langmuir **27**, 4048 (2011).

[50] S.-H. Chen and E. Y. Sheu, J. Appl. Cryst. **21**, 751 (1988).